ELSEVIER

Journal of Organometallic Chemistry 582 (1999) 16–24

Journal of Organometallic Chemistry

Synthesis and structural features of new sterically hindered azaphosphatrane systems: $ZP(RNCH_2CH_2)_3N$☆

X. Liu, Y. Bai, J.G. Verkade *

Department of Chemistry, Iowa State University, Ames, IA 50011, USA

Received 14 August 1998

Abstract

The synthesis of $[ZP(RNCH_2CH_2)_3N]CF_3SO_3$ wherein $Z = H^+$ and $R = SiMe_3$ (**1f**), $SiEt_3$ (**1g**), $SiPh_3$ (**1h**), $SiPh_2Me$ (**1i**) and Li (**1j**), are reported along with that of **2f** wherein Z = lp and $R = SiMe_3$. Also described are the transformations of **1j** to **1f–i**, **2f** to $OP(Me_3SiNCH_2CH_2)_3N$ (**3b**), **5** to **3b**, and **2f** to $SP(Me_3SiNCH_2CH_2)_3N$ (**3a**). The structures of **2f** and **3a** determined by X-ray means are also presented. Compound **2f** displays a bridgehead–bridgehead distance of 3.360(7) Å while that in **3a** is 3.152(7) Å. The smaller distance in the latter by ca. 0.1 Å is attributed to the wider NPN bond angle by ca. 5° in **3a**. VT ^{31}P-NMR studies revealed no evidence for transannulation or tautomerism in **3b**.

Keywords: Azaphosphatrane; Steric hindrance; Transannulation

1. Introduction

In recent years we have been exploring the chemistry of azaphosphatranes such as **1a–e**, particularly as it is related to the deprotonated parents of these cations, namely, their corresponding proazaphosphatranes 2**a–e** [1–14].

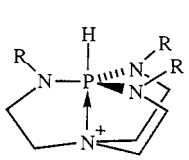

	R	
1a	H	**2a**
1b	Me	**2b**
1c	Et	**2c**
1d	*i*-Pr	**2d**
1e	Bn	**2e**
1f	$SiMe_3$	**2f**
1g	$SiEt_3$	**2g**
1h	$SiPh_3$	
1i	$SiPh_2Me$	
1j	Li	

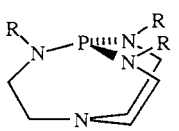

Some of these proazaphosphatranes are proving to be exceedingly potent catalysts, promoters and strong nonionic bases that facilitate a variety of useful organic transformations. For example, **2b** is a superior catalyst for the trimerization of aryl and alkyl isocyanates to isocyanurates (Eq. (1)) that are useful as additives in the manufacture of Nylon-6 [1]. Compound **2b** is a superior catalyst for the protective silylation of a wide variety of sterically hindered and deactivated alcohols [12], and it is also an excellent promoter for the acylation of such substrates [10].

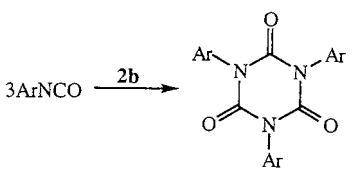

(1)

Proazaphosphatrane **2b** is 17 p*K* units stronger as a base than DBU [2], a commonly used nonionic base in organic synthesis. Thus **2b** has facilitated a substantial improvement in the synthesis of porphyrins [5], the dehydrohalogenation of secondary and tertiary halides [14] and in the synthesis of a chiral

☆ Dedicated to Alan Cowley on the occasion of his 65th birthday.

* Corresponding author.

0022-328X/99/$ - see front matter
PII: S0022-328X(98)01180-2

fluorescence agent [15]. As a result of these as well as currently emerging applications, **2b** has become commercially available [16].

All of these transformations are crucially dependent upon the ability of the bridgehead nitrogen in **2b** to form a partial or full coordinate bond to the phosphorus [17]. In support of this hypothesis we observed, for example, that the acyclic analogue $P(NMe_2)_3$ is ineffective in all of the aforementioned reactions.

The first proazaphosphatrane for which we were able to obtain crystals suitable for an X-ray structural study was **2d**. A curious feature we observed in this structure is the virtually planar geometry around the bridgehead nitrogen (angle sum = 358.7°) [8]. This geometry was attributed to van der Waals repulsions among the methylene protons adjacent to the bridgehead nitrogen, which tended to draw the nitrogen from a downwardly directed pyramidal sp^3 geometry into a nearly planar sp^2 hybridized geometry. The planarity of the bridgehead nitrogen is mainly responsible for the transannular N–P distance of 3.29 Å in **2d** which is only about 2% shorter than the van der Waals sum of 3.35 Å [8].

With the above considerations in mind, we sought to synthesize and structurally characterize a proazaphosphatrane that engenders even greater steric encumbrance around the phosphorus than **2d**, in order to determine if the bridgehead–bridgehead distance would be elongated, and if so, whether the bridgehead nitrogen would be more pyramidal, or the NPN bond angles (angle sum = 309.7(7)° in **2d**) would be sterically compressed.

Here we report the synthesis of **1f–j** and of **2f**, and the conclusion from the X-ray structure of **2f** that although its transannular distance is slightly [0.06(1) Å] longer than that in **2d**, both bridgehead bond angle sums are unchanged from those in **2d**. Also described are the conversions of **1j** to **1f–i**, **2f** to **3b**, **5** to **3b** and **2f** to **3a**. Evidence is also presented for the formation of **6**(CF_3SO_3) in the synthesis of **1f**. The molecular structural parameters for **3a** determined herein by X-ray means, are compared with those determined earlier for **4** [18].

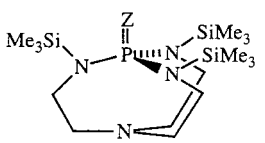

3a: Z = S
3b: Z = O

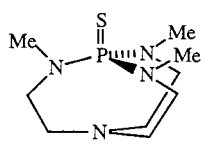

4

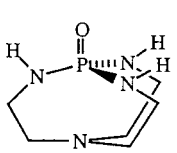

5

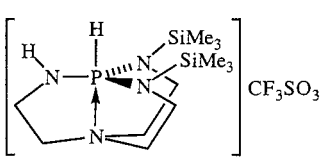

6

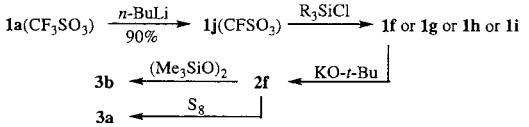

Scheme 1.

2. Results and discussion

2.1. Syntheses

Although the trilithio azaphosphatrane **1j**(CF_3SO_3) could be isolated in 90% yield via step 1 in Scheme 1, compounds **1f–i** derived from **1j**(CF_3SO_3) by silylation in step 2 of this scheme were obtained in better yields and with greater convenience by generating **1j** in situ followed by trisilylation. In view of the relative ease with which trisilylation of **1j**(CF_3SO_3) occurred to give the corresponding salts **1g–i** (51–63% yield) it was surprising to observe that **1j** upon reaction with Me_3SiCl (the least sterically hindered silylating agent employed) gave rise to a 3:1 mixture of the desired product **1f** and what is probably **6**(CF_3SO_3) the disilylated product. Evidence for the latter compound is its ^{31}P chemical shift (-34.3 ppm) which is upfield as is the case for cation **7** (-23.2 ppm [8]).

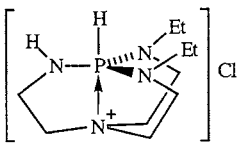

7

The reason(s) for the incomplete silylation here are not obvious. Attempts to deprotonate **1f–i** with KO*t*-Bu, the base of choice for these strong nonionic bases, succeeded only in the case of **1f**(CF_3SO_3). For reasons that are not clear severe decomposition occurred when **1g–i** were treated with KO*t*-Bu.

Proazaphosphatrane **2f**, obtained in 58% overall yield from **1a**(CF_3SO_3), was oxidized to **3b** with $(Me_3SiO)_2$ (Scheme 1) in 94% yield. The oxide **3b** was also derived from **5** in 51% overall yield according to Scheme 2, presumably via intermediate **8** which was not isolated. Proazaphosphatrane **2f** reacts with sulfur as shown in Scheme 1 to give crystalline **3a** in 76% yield.

We had previously synthesized **5** from **1a** by allowing the latter to react with molecular oxygen [18]. The yield of **5** was improved here (71%) over that reported earlier (48% [18]) by reacting **1a** with $(Me_3SiO)_2$.

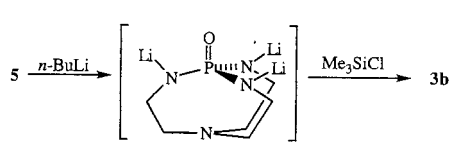

8

Scheme 2.

Table 1
^{31}P-NMR chemical shifts for protonated pro-azaphosphatranes $HP(RNCH_2CH_2)_3N^+$

R[a]	Number of R groups ≠ H	δ^{31}P (ppm)[b]	Ref.
(**1a**)	0	−45.2	–[e]
Me (**1b**)	3	−10.0[c]	[18]
Me	2	−21.4[c]	[18]
Me	1	−35.5[c]	[18]
Et (**1c**)	3	−13.5[d]	[8]
Et	2	−23.2[d]	[8]
Et	1	−33.6[d]	[8]
i-Pr (**1d**)	3	−11.8[d]	[8]
i-Pr	2	−21.7[d]	[8]
i-Pr	1	−32.3[d]	–[f]
$PhCH_2$ (**1e**)	3	−11.0[d]	–[e]
Me_3Si (**1f**)	3	−24.5	This work
Me_3Si	2	−34.3	This work
Me_3Si	1	−42.0	This work
Et_3Si (**1g**)	3	−25.9	This work
Et_3Si	2	−38.8	This work
Et_3Si	1	−43.0	This work
Ph_3Si (**1h**)	3	−19.6	This work
Ph_3Si	2	−36.0	This work
Ph_3Si	1	−42.4	This work
$MePh_2Si$ (**1i**)	3	−34.3	This work
$MePh_2Si$	2	−39.3	This work
$MePh_2Si$	1	−43.1	This work

[a] R is defined here as a substituent other than hydrogen. Thus **1a** possesses a hydrogen on each equatorial nitrogen.
[b] Chemical shifts were measured in CD_3CN unless stated otherwise.
[c] DMSO.
[d] $CDCl_3$.
[e] M.A.H. Laramay, J.G. Verkade, J. Am. Chem. Soc. 112 (1990) 9421.
[f] P.B. Kisanga, J.G. Verkade, to be published.

2.2. NMR studies

A plot of the ^{31}P chemical shifts of protonated pro-azaphosphatranes (summarized in Table 1) against the degree of R substitution for hydrogen shown in Fig. 1 reveals some interesting trends. Trisubstituted alkyl and benzyl species display a comparatively narrow (~4 ppm) δ^{31}P range (which is downfield) relative to their silyl counterparts (~14 ppm). These relationships, though largely preserved, become less pronounced as the number of non-hydrogen R groups decreases. Interestingly, the δ^{31}P values progress upfield with decreasing R substitution until the value of −45.2 ppm is reached when all the R groups are replaced by hydrogens (**1a**). The trisubstituted lithium compound **1j** displays a δ^{31}P value (−17.7 ppm) that lies between the ranges for its trialkyl and trisilyl analogues. The orders in the δ^{31}P values at each level of R substitution do not follow an obvious trend.

In efforts to determine if the Me_3Si groups on **3b** are sufficiently electronegative (via N→Si π-bonding effects) to induce sufficient transannulation (i.e. **3′b**) to affect the ^{31}P-NMR chemical shift, and also to see whether evidence for tautomer **3″b** could be found (owing to the superior strength of the Si–O bond and perhaps steric congestion among the equatorial Me_3Si groups) VT ^{31}P- and ^{1}H-NMR studies were carried out.

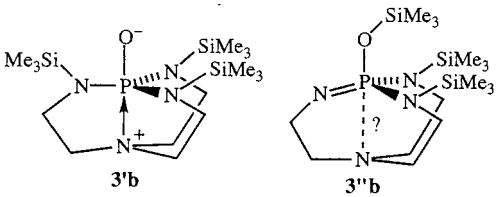

3′b **3″b**

It was observed that the position of the ^{31}P peak is independent of temperature, although the ^{1}H-NMR spectrum of compound **3b** is temperature dependent. At 298 K, the resonance of the methylene protons showed two sets of multiplets (2.00–2.30 and 2.40–2.80 ppm). With increasing temperature, the peaks in the 2.00–2.30 ppm range began to combine with some of the peaks in 2.40–2.80 ppm range to form a broad peak at ca. 2.42 ppm, while the remaining peaks in 2.40–2.80 ppm range became sharper. At 343 K, the resonance of the methylene protons showed one broad peak at 2.42 ppm and one appearing to be a doublet of triplets at 2.79 ppm. It is suggested that at lower temperatures, compound **3b** is rigid due to slow conformational inversion of the rings. Thus the protons of the methylene groups are not equivalent, displaying separated multiplet character in the ^{1}H-NMR spectrum. At higher temperatures, the structure becomes more flexible, rendering the protons of the methylene groups equivalent on the NMR time scale, thus accounting for the appearance of one doublet of triplets.

Efforts to compare the basicities of **1g**(CF_3SO_3) and **1h**(CF_3SO_3) with **2b** were partially successful. ^{31}P-NMR monitoring of reactions 2 and 3 in CD_3CN showed that for reaction 2

$$\mathbf{1g}(CF_3SO_3) + \mathbf{2b} \rightleftharpoons \mathbf{2g} + \mathbf{1b} \quad (2)$$

$$\mathbf{1h}(CF_3SO_3) + \mathbf{2b} \rightleftharpoons \mathbf{2h} + \mathbf{1b} \quad (3)$$

in CD_3CN, **1b** (along with its P–D analogue) and **2g** (101 ppm) were formed, as well as **9** (97.0 ppm) owing to hydrolysis by adventitious water. In an analogous reaction of **1b** and **2b**, **1b** (along with its P–D analogue) and **2h** ($\delta^{31}P = 105$ ppm) were formed, as well as some partially hydrolyzed product **10** ($\delta^{31}P = 99.1$ ppm).

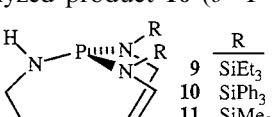
9

	R
9	$SiEt_3$
10	$SiPh_3$
11	$SiMe_3$

Both experiments suggest, however, that **2b** is more basic than **2g** or **2h**. Although these equilibria lie far to the right, the extreme sensitivity of **2g** and **2h** to moisture, made calculation of an equilibrium constant unwarranted.

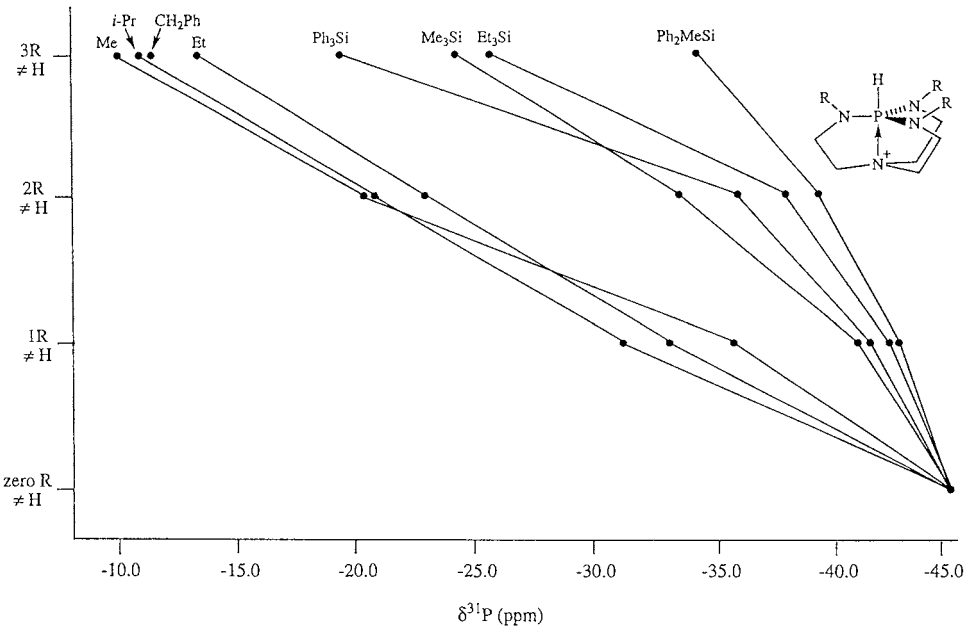

Fig. 1. Plot of ^{31}P-NMR chemical shifts of protonated pro-azaphosphatranes against the number of non-hydrogen R groups.

This moisture sensitivity was also shown for **2f** (Fig. 2) by monitoring its ^{31}P-NMR spectrum upon treatment with three equivalents of H_2O in CD_3CN (see Section 3). The results are summarized in Scheme 3. Some support for the lack of formation of **1f**(OH) in the first step of this scheme is the absence of a ^{31}P-NMR peak at -24.5 ppm and the persistence of cation **12** for up to 1 week. The reduced hydrolytic sensitivity of cations such as **1f**, **12** and **13** may be attributed to the presence of $N_{ax} \rightarrow P$ transannulation that reduces the electrophilicity of the silicon substituents. By contrast, untransannulated **3a** (Fig. 3) hydrolyzes completely to **5** in 2 h at room temperature as shown by its ^{31}P, ^{1}H and mass spectra, which compared favorably to data we published earlier [19].

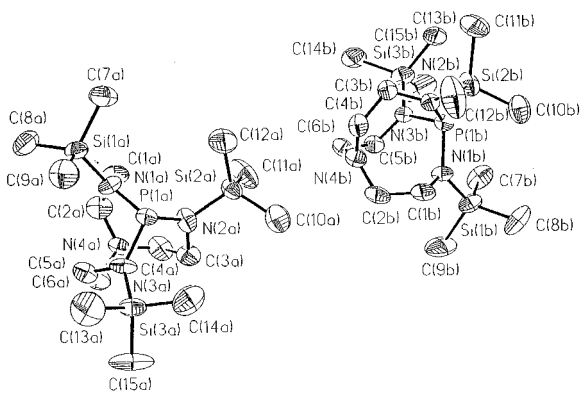

Fig. 2. Computer drawing of **2f** with thermal ellipsoids at the 50% probability level.

2.3. Structural considerations

Compound **2f** is only the second pro-azaphosphatrane that has thus far provided crystals suitable for X-ray analysis, the first being **1d** [8]. The bridgehead–bridgehead distances in these two compounds (**2f**, avg 3.360(7) Å; **2d**, 3.293(2) Å), average NPN angles (**2f**, 103.3(2)°; **2d**, 103.24(7)°) and average CNC angles (**2f**, 119.3(5)°; **2d**, 119.6(2)°) are quite comparable. Thus any changes in stereoelectronic effects have a minimal effect on the overall geometry of the cage core.

Compound **3a** (Fig. 3) is only the second pro-azaphosphatrane sulfide in addition to **8** to have been structured by X-ray means. The bridgehead–bridgehead distances (**3a**, 3.152(7); **8**, 3.177(4) Å), average NPN angles (**3a**, 107.9(2)°); **8**, 106.7(1)°) and average CNC angles (**3a**, 119.8(5)°; **8**, 119.4(3)°) are again very comparable, as are the P–S distances (**3b**, 1.952(2) Å; **8**, 1.957(1) Å).

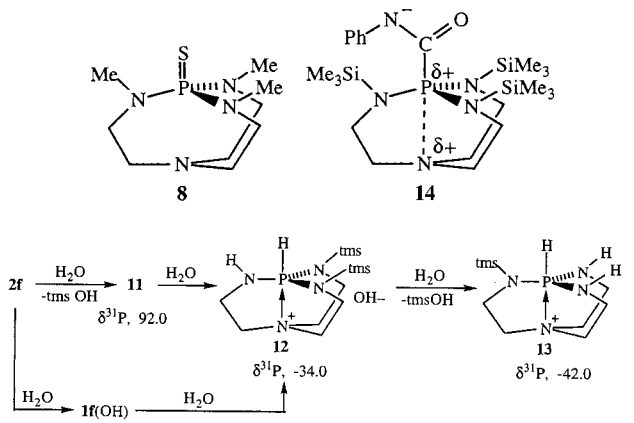

Scheme 3.

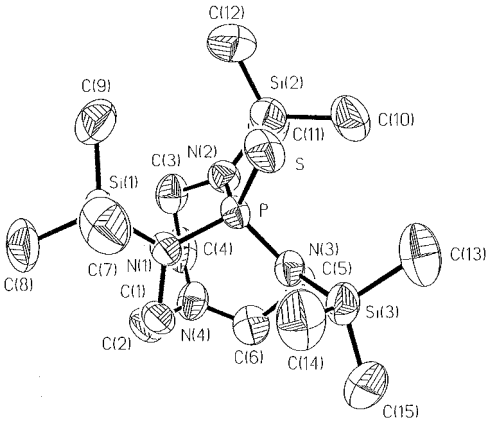

Fig. 3. Computer drawing of **3a** with thermal ellipsoids at the 50% probability level.

The smaller bridgehead–bridgehead distance by ca. 0.27 Å in **2f** compared with **3a** appears to be associated with the wider NPN angle in the latter compound (by ca. 5°) which tends to lift the nearly planar bridgehead nitrogen somewhat more strongly toward the phosphorus.

2.4. Catalytic properties of *2f*

Like **2b** [1] and **2d** [8], **2f** is a potent catalyst for reaction 1 in which Ar = Ph. Thus at r.t., PhNCO is exothermically trimerized to the corresponding phenyl isocyanurate at r.t. in 97% yield. This result demonstrates that the zwitterionic intermediate **14**, like its analogue of **2b** [1] and of **2d** [8], can form despite the formidable steric bulk provided by the $SiMe_3$ groups.

3. Experimental

3.1. General procedures

Acetonitrile and benzene were dried with CaH_2, and THF, toluene, and pentane were dried with sodium. All solvents were freshly distilled from their respective drying agents and all reactions were carried out under argon. ^{1}H- and ^{13}C-NMR spectra were recorded on a Varian VXR-300 NMR spectrometer or a Bruker WM-200 NMR spectrometer. ^{31}P-NMR spectra were recorded on a Bruker WM-200 NMR spectrometer using 85% H_3PO_4 as the external standard. High-resolution mass spectra were recorded on a KRATOS MS-50 spectrometer and ESI mass spectra were performed using a FINNIGAN TSQ700 spectrometer. Elemental analysis were performed in the Instrument Services Laboratory of the Chemistry Department at Iowa State University. Compounds **1a**(CF_3SO_3) [19] and **2b** [20] were synthesized according to our previously published methods.

3.2. [HP(LiNCH$_2$CH$_2$)$_3$N](CF$_3$SO$_3$), *1j*(CF$_3$SO$_3$)

A suspension of **1a**(CF_3SO_3) (0.324 g, 1.00 mmol) in THF (50 ml) was cooled to −78°C under argon. *N*-Butyllithium (1.28 ml, 3.20 mmol) as a 2.5 M solution in hexane was added and the reaction mixture was stirred while it warmed slowly to r.t. Stirring was continued for 4 h at r.t. The volatiles were then removed in vacuo and the residue was washed with cold (0°C) pentane (20 ml). After drying the residue in vacuo, **1j**(CF_3SO_3) was obtained as a white powder (3.10 g, 90%) and was used in the following reaction without further purification. Attempts to purify this compound consistently resulted in less pure material. ^{31}P (CD_3CN): δ −17.67 (bds). ^{1}H (CD_3CN): δ 2.59 − 2.80 (bdm, 12H, $N_{eq}CH_2$ and $N_{ax}CH_2$ resonances overlapped), 6.27 (d, 1H, PH, $^1J_{PH}$ = 460 Hz). ^{13}C (CD_3CN): δ 37.62 (bds, $N_{ax}CH_2$), 50.63 (bds, $N_{eq}CH_2$).

3.3. [HP(Me$_3$SiNCH$_2$CH$_2$)$_3$N](CF$_3$SO$_3$), *1f*(CF$_3$SO$_3$)

Both isolated **1j**(CF_3SO_3) and **1j**(CF_3SO_3) generated in situ used in this reaction gave similar results. Here the procedure for the preparation of **1f**(CF_3SO_3) using **1j**(CF_3SO_3) synthesized in situ as a starting material is described and the in situ method is also employed in subsequent preparations. A suspension of **1j**(CF_3SO_3) generated in situ from **1a**(CF_3SO_3) (3.24 g, 10.0 mmol) in THF (300 ml) was cooled to −78°C under argon. Trimethylsilyl chloride (4.37 g, 40.0 mmol) was slowly added with a syringe. The mixture (in a flask closed by a septum) was allowed to warm slowly to r.t. and was stirred at that temperature for an additional 10 h. The volatiles were removed in vacuo and the residue was extracted with acetonitrile (3 × 25 ml). The extract was filtered and the solvent was removed in vacuo to give a powder which was washed with pentane (1 × 50 ml). The ^{31}P- and ^{1}H-NMR spectra of this white powder in CD_3CN indicated that a mixture of **1f**(CF_3SO_3) and **5**(CF_3SO_3) was formed in a ca. 3:1 ratio (see Section 2). The ratio of trimethylsilyl chloride was increased to six equivalents and the reaction time was extended from 10 to 48 h in an attempt to synthesize pure **1f**(CF_3SO_3). However, the product mixture ratio remained unchanged. Although attempts to isolate pure **1f**(CF_3SO_3) from this mixture were not successful, the mixture was used in the following reaction to prepare **2f**.

3.4. P(Me$_3$SiNCH$_2$CH$_2$)$_3$N, *2f*

A suspension of 1.05 g of the above-described mixture of **1f**(CF_3SO_3) and **5**(CF_3SO_3) in THF (80 ml) was added to a suspension of KO*t*-Bu (0.336 g, 3.00 mmol) in THF (20 ml) at r.t. After the reaction mixture was stirred for 2 h at r.t., the volatiles were removed in vacuo and the residue was extracted with toluene (1 ×

Table 2
Crystallographic data for **2f** and **3a**

Empirical formula	$C_{15}H_{39}N_4PSi_3$	$C_{15}H_{30}N_4PSSi_3$
Formula weight	390.74	413.73
Crystal color, habit	Clear, rectangular	Colorless plate
Crystal size (mm)	$0.4\times0.2\times0.2$	$0.4\times0.3\times0.08$
Crystal system	Triclinic	Monoclinic
Reflections used for unit cell determination (2θ-range)	25 (18–31°)	25 (4.27–15.77°)
Unit cell dimensions		
a (Å)	10.304(5)	17.841(4)
b (Å)	14.963(7)	9.532(2)
c(Å^3)	16.753(8)	15.611(3)
α (°)	78.51(4)	111.38(3)
β (°)	86.66(4)	2397.2(20)
γ (°)	71.28(3)	
Space group	$P\bar{1}$	$P2_1/n$
Z	4	4
$D_{calc.}$ (g cm^{-3})	1.083	1.112
μ(Cu–K$_\alpha$) (mm^{-1})	2.479	0.347
Diffractometer	Siemens P4	Enraf-Nonius CAD4
Radiation, graphite monochromated	Cu–K$_\alpha$ ($\lambda = 1.54178$ Å)	Mo–K$_\alpha$ (0.71073 Å)
Temperature (K)	213(2)	293(2)
Scan type	$2\theta{:}\theta$	ω-2θ
$2\theta_{max}$	108.74	54.94
Reflections measured	5884	5664
Corrections	Lorentz-polarization absorption (trans. factors 0.708–0.814)	Lorentz-polarization absorption (trans. factors 0.758–0.626)
Reflections observed [$I>2\sigma(I)$]	4208	2230
Number of variables	415	217
Residuals: R, R_w[a]	0.0699, 0.1830	0.0777, 0.1573
Goodness-of-fit indicator[b]	1.113	1.191
Max. shift/error in final cycle	0.000	0.000
Max., min. difference peak (e Å^{-3})	0.690	0.430

[a] $R = \Sigma||F_o|-|F_c||/\Sigma|F_o|$; $R_w = [\Sigma w(|F_o|-|F_c|)^2/\Sigma w|F_o|]^{1/2}$.
[b] Goodness of fit, $[w(|F_o|-|F_c|^2/(n_{obs}-n_{par})]^{1/2}$.

50 ml). The extract was filtered and the solvent was removed in vacuo. Colorless crystalline **2f** was obtained upon sublimation at 80°C/0.5 Torr (0.451 g, 58% overall yield based on **1a**). ^{31}P (C_6D_6): δ 99.67. ^{1}H (C_6D_6): δ 0.24 (d, 27H, CH_3, $^4J_{PH} = 3.0$ Hz), 2.68 (bdm, 12H, $N_{eq}CH_2$ and $N_{ax}CH_2$ overlapped). ^{13}C (C_6D_6): δ 1.18 (d, CH_3, $^3J_{PC} = 9.0$ Hz), 40.95 (d, $N_{eq}CH_2$, $^2J_{PC} = 4.5$ Hz), 54.93 (d, $N_{ax}CH_2$, $^3J_{PC} = 3.0$ Hz). HRMS m/z calculated for $C_{15}N_{39}N_4Si_3P$: 390.22202. Found: 390.22155 (27.1, M^+). Anal. Calc. for $C_{15}H_{39}N_4Si_3P$: C, 46.11; H, 10.06; N, 14.34. Found: C, 45.40; H, 10.21; N, 14.44%.

3.5. *[HP(Et$_3$SiNCH$_2$CH$_2$)$_3$N](CF$_3$SO$_3$)*, ***1g**(CF$_3$SO$_3$)*

The synthesis of **1g**(CF_3SO_3) was analogous to that of **1f**(CF_3SO_3) except that triethylsilyl chloride (4.55 g, 40.0 mmol) was used instead of trimethylsilyl chloride. The product **1g**(CF_3SO_3) was obtained as a white powder (4.02 g, 60%). ^{31}P (CD_3CN): δ −25.99. ^{1}H (CD_3CN): δ 0.80 (q, 18H, $N_{eq}Si(CH_2CH_3)_3$, $^3J_{HH} = 8.0$ Hz), 0.98 (t, 27H, $N_{eq}Si(CH_2CH_3)_3$, $^3J_{HH} = 8.0$ Hz), 2.85 (bdm, 6H, $N_{ax}CH_2$), 3.03 (dt, 6H, $N_{eq}CH_2$, $^3J_{PH} = 16.0$ Hz, $^3J_{HH} = 6.0$ Hz), 6.28 (d, 1H, PH, $^1J_{PH} = 504$ Hz). ^{13}C (CD_3CN): δ 5.14 (d, CH_2CH_3, $^3J_{PC} = 2.5$ Hz), 7.65 (s, CH_2CH_3), 38.52 (s, $N_{ax}CH_2$), 52.84 (d, $N_{eq}CH_2$, $^2J_{PC} = 11.1$ Hz). MS (ESI) m/z: 517.2 (cation **1g**).

3.6. *[HP(Ph$_3$SiNCH$_2$CH$_2$)$_3$N](CF$_3$SO$_3$)*, ***1h**(CF$_3$SO$_3$)*

The synthesis of **1h**(CF_3SO_3) was analogous to that of **1f**(CF_3SO_3) except that triphenylsilyl chloride (11.8 g, 40.0 mmol) was used instead of trimethylsilyl chloride. The product **1h**(CF_3SO_3) was obtained as a white powder (5.61 g, 51%). ^{31}P (CD_3CN): δ −19.64. ^{1}H (CD_3CN): δ 2.88 (bdm, 6H, $N_{ax}CH_2$), 3.58 (dt, 6H, $N_{eq}CH_2$, $^3J_{PH} = 16.0$ Hz, $^3J_{HH} = 6.0$ Hz), 6.92 (d,1H, PH, $^1J_{PH} = 532$ Hz), 7.07–7.49 (m, 45H, C_6H_5). ^{13}C (CD_3CN): δ 42.57 (s, $N_{ax}CH_2$), 52.07 (d, $N_{eq}CH_2$, $^2J_{PC} = 10.0$ Hz), 129.35 (s, C_6H_5), 131.64 (s, C_6H_5), 132.43 (d, C_6H_5, $^3J_{PC} = 1.5$ Hz), 137.29 (s, C_6H_5). MS (ESI) m/z: 949.1 (cation **1h**). Anal. Calc. for $C_{61}H_{58}N_4Si_3O_3PSF_3$: C, 66.64; H, 5.32; N, 5.10. Found: C, 66.87; H, 5.68; N, 4.87%.

Table 3
Selected bond angles and bond distances in **2f**

Bond angles (°)			
N(3A)–P(1A)–N(2A)	103.1(2)	N(1B)–P(1B)–N(2B)	103.8(2)
N(3A)–P(1A)–N(1A)	102.6(2)	N(1B)–P(1B)–N(3B)	103.4(2)
N(2A)–P(1A)–N(1A)	104.2(2)	N(2B)–P(1B)–N(3B)	102.7(2)
C(4A)–N(4A)–C(6A)	120.6(5)	C(4B)–N(4B)–C(6B)	119.8(5)
C(4A)–N(4A)–C(2A)	119.9(5)	C(4B)–N(4B)–C(2B)	118.7(5)
C(6A)–N(4A)–C(2A)	117.8(5)	C(6B)–N(4B)–C(2B)	119.1(5)
Bond lengths (Å)			
P(1A)–N(3A)	1.705(5)	Si(1A)–N(1A)	1.735(5)
P(1A)–N(2A)	1.715(5)	Si(2A)–N(2A)	1.737(5)
P(1A)–N(1A)	1.711(5)	Si(3A)–N(3A)	1.732(5)
P(1B)–N(1B)	1.711(4)	Si(1B)–N(1B)	1.745(5)
P(1B)–N(2B)	1.715(4)	Si(2B)–N(2B)	1.747(4)
P(1B)–N(3B)	1.720(4)	Si(3B)–N(3B)	1.730(4)

3.7. *[HP(Ph$_2$MeSiNCH$_2$CH$_2$)$_3$N](CF$_3$SO$_3$)*, ***1i**(CF$_3$SO$_3$)*

The synthesis of **1i**(CF_3SO_3) was analogous to that of **1f**(CF_3SO_3) except that diphenylmethylsilyl chloride (9.72 g, 40.0 mmol) was used instead of trimethylsilyl chloride. The product **1i**(CF_3SO_3) was obtained as a white powder (5.45 g, 63%). ^{31}P (CD_3CN): δ −34.25. ^{1}H (CD_3CN): δ 0.42 (d, 9H, CH_3, $^4J_{PH} = 1.8$ Hz), 2.97–3.21 (m, 12H, $N_{eq}CH_2$ and $N_{ax}CH_2$ overlapped), 6.65 (d, 1H, PH, $^1J_{PH} = 494$ Hz), 7.35–7.52 (m, 30H, C_6H_5). ^{13}C (CD_3CN): δ −0.98 (d, CH_3, $^3J_{PC} = 3.1$ Hz), 40.25 (s, $N_{ax}CH_2$), 50.62 (d, $N_{eq}CH_2$, $^3J_{PC} = 11.6$ Hz), 129.50 (s, C_6H_5), 131.62 (s, C_6H_5), 135.10 (s, C_6H_5), 135.64 (s, C_6H_5). MS (ESI) m/z: 762.9 (cation **1i**).

3.8. *S=P(Me$_3$SiNCH$_2$CH$_2$)$_3$N*, ***3a***

Elemental sulfur (0.039 g, 1.20 mmol) was added to a solution of **2f** (0.390 g, 1.00 mmol) in benzene (20 ml) at 0°C. After stirring the reaction mixture for 12 h at r.t., it was filtered and the solvent in the filtrate was slowly evaporated to give product **3b** as a colorless crystalline solid (0.332 g, 76%). ^{31}P (C_6D_6): δ 65.30. ^{1}H (C_6D_6): δ 0.44 (s, 27H, CH_3), 2.11–2.26 and 2.53–2.82 (bdm, 12H, $N_{eq}CH_2$ and $N_{ax}CH_2$ overlapped). ^{13}C (C_6D_6): δ 2.55 (s, CH_3), 47.34 (d, $N_{eq}CH_2$, $^2J_{PC} = 3.0$ Hz), 55.00 (s, $N_{ax}CH_2$). HRMS m/z calculated for $C_{15}H_{39}N_4SPSi_3$: 422.19410. Found: 422.19367 (37.8, M^+). Anal. Calc. for $C_{15}H_{39}N_4SPSi_3$: C, 42.61; H, 9.30; N, 13.25. Found: C, 42.89; H, 9.43; N, 13.15.

Table 4
Selected bond angles and distances in **3a**

Bond angles (°)			
N(2)–P–N(3)	107.9(2)	N(1)–P–S	110.7(2)
N(2)–P–N(1)	107.9(2)	C(4)–N(4)–C(6)	120.1(6)
N(3)–P–N(1)	107.9(2)	C(4)–N(4)–C(2)	119.4(5)
N(2)–P–S	111.6(2)	C(6)–N(4)–C(2)	119.8(5)
N(3)–P–S	110.8(2)		
Bond lengths (Å)			
P–N(2)	1.653(5)	P–N(1)	1.675(4)
P–N(3)	1.661(5)	P–S	1.952(2)

3.9. *O=P(Me$_3$SiNCH$_2$CH$_2$)$_3$N*, ***3b***

3.9.1. Method A

Bistrimethylsilyl peroxide (0.214 g, 1.20 mmol) was added to a solution of **2f** (0.390 g, 1.00 mmol) in pentane (20 ml) at 0°C. After 10 h at r.t., the reaction mixture was filtered and the solvent was evaporated in vacuo to give **3b** as a white solid (0.340 g, 84%) which was further purified by sublimation at 80°C/0.5 Torr. (0.321 g, 94%). ^{31}P (C_6D_6): δ 24.11. ^{1}H (C_6D_6): δ 0.34 (d, 27H, CH_3, $^4J_{PH} = 3.0$ Hz), 2.14–2.71 (bdm, 12H, $N_{eq}CH_2$ and $N_{ax}CH_2$). ^{13}C (C_6D_6): δ 1.58 (d, CH_3, $^3J_{PC} = 1.5$ Hz), 47.16 (d, $N_{eq}CH_2$, $^2J_{PC} = 2.3$ Hz), 54.96 (s, $N_{ax}CH_2$). HRMS m/z calculated for $C_{15}H_{39}N_4Si_3PO$: 406.21694. Found: 406.21209.

3.9.2. Method B

A suspension of **5** (0.190 g, 1.00 mmol) in THF (50 ml) was cooled to −78°C under argon. *N*-Butyllithium (1.28 ml, 3.20 mmol) as a 2.5 M solution in hexane was then added with a syringe and after 30 min the reaction mixture was allowed to warm slowly to r.t. where it was stirred for an additional 3 h. The reaction mixture was then cooled to −78°C and trimethylsilyl chloride (0.443 g, 4.00 mmol) was slowly added. The reaction mixture was again allowed to warm slowly to r.t. where it was stirred for an additional 12 h. All the volatiles were then removed in vacuo and the residue was extracted with toluene (1×50 ml). The extract was filtered through Celite and the toluene in the filtrate was removed in vacuo. The residue was sublimed at 80°C/0.5 Torr to give product **3b** as a white solid (0.212 g, 51%).

3.10. *O=P(HNCH$_2$CH$_2$)$_3$N*, ***5***

Although we reported this compound previously [19], we found that the action of bistrimethylsilyl peroxide instead of molecular oxygen on **1a** gave a higher yield of **5** in less time. To a suspension of **1a**(CF_3SO_3) (3.24 g, 10.0 mmol) in THF (150 ml) at r.t. was added a solution of KO*t*-Bu (1.35 g, 12.0 mmol) in acetonitrile (20 ml) followed by the addition of bistrimethylsilyl peroxide (2.02 g, 12.0 mmol) over a period of 10 min.

The reaction mixture was stirred at r.t. for 12 h and then filtered. The crude product was obtained as a yellowish solid from the filtrate by evaporation in vacuo. Compound **5** (1.35 g, 71%, lit. 48% [19]) was recrystallized from methanol as colorless crystals. The ^{31}P-, ^{1}H-, ^{13}C-NMR and mass spectral data were consistent with those in the literature [19].

3.11. Hydrolysis of *2f*

Water (6 ml, 0.3 mmol) was added at r.t. via syringe to a solution of **2f** (40 mg, 0.10 mmol) in CD_3CN (0.6 ml) in an NMR tube. After shaking the NMR tube for 1 min, the reaction mixture was allowed to stand at r.t. A ^{31}P-NMR spectrum of the reaction mixture was taken 30, 90 and 480 min after the reagents had been mixed. After 30 min, the ^{31}P-NMR spectra showed, that in addition to decreased signal intensity for the starting material **2f**, there appeared a new signal at 92.0 ppm and a triplet at -33.0 ppm whose members were of equal intensity. After 90 min, the signal for the starting material vanished completely, the signal at 92.0 ppm decreased and the triplet, now at -35.0 ppm, greatly increased. After 480 min, the signals at 92.0 and -35.0 ppm disappeared while a new signal at -42.0 ppm was observed that persisted for a week (see Section 2).

3.12. Catalytic trimerization of PhNCO by *2f*

To a solution of **2f** (0.41 g, 1.0 mmol) in dry benzene (20 ml) under argon was added (by syringe) phenyl isocyanate (6.00 g, 99% pure, 50.0 mmol, Aldrich). After the mixture was stirred at r.t. for 2 min, a white precipitate rapidly formed, transforming the reaction mixture into a solid mass. The solid was allowed to cool to r.t. and 30 ml of dry benzene was added. After stirring at r.t. for 1 h, the resulting suspension was filtered in vacuo, further washed with 15 ml of dry benzene, and finally dried in vacuo to give phenyl isocyanurate as a white solid (5.82 g, 97%). The ^{1}H- and ^{13}C-NMR and mass spectroscopic data matched those in the literature [6].

3.13. ^{1}H-VTNMR of $O{=}P(Me_3SiNCH_2CH_2)_3N$, *3b*

Solutions of **3b** (41 mg, 0.10 mmol) in CD_3CN (0.6 ml) and C_6D_6 (0.6 ml) were prepared. ^{31}P-NMR spectra of **3a** in CD_3CN were taken at 251, 261, 293, 323 and 341 K. ^{1}H-NMR spectra of **3a** in C_6D_6 were also taken at 298, 323, and 343 K.

3.14. X-ray structural determinations of *2f* and *3a*

A crystal of **2f** was mounted on a glass fiber on the Siemens P4 for data collection at $213(2) \pm 1$ K. The cell constants for the data collection were determined from reflections found from a 360° rotation photograph. A total of 25 reflections in the range of 18–31° θ were used to determine precise cell constants. Pertinent data collection and reduction information are given in Table 2. Lorentz and polarization corrections and a nonlinear correction based on the decay in the standard reflections were applied to the data. A series of azimuthal reflections was collected and a semi-empirical absorption correction was applied to the data. The space group $P\bar{1}$ was chosen based on systematic absences and intensity statistics. This assumption proved to be correct as determined by a successful direct-methods solution [21] and subsequent refinement. All non-hydrogen atoms were placed directly from the E-map. All non-hydrogen atoms were refined with anisotropic displacement parameters and all hydrogens were treated as riding-atoms with individual isotropic displacement parameters. Final refinements were carried out [21–23]. Selected bond angles and distances are collected in Table 3.

A crystal of **3a** was mounted on a glass fiber on the Enraf-Nonius CAD4 for data collection at $293(2) \pm 1$ K. The cell constants for the data collection were determined from reflections found from a 360° rotation photograph. A total of 25 reflections in the range of 4.27–15.77° θ were used to determine precise cell constants. Pertinent data collection and reduction information is given in Table 2. Lorentz and polarization corrections and a nonlinear correction based on the decay in the standard reflections were applied to the data. A series of azimuthal reflections was collected for this specimen and a semi-empirical absorption correction was applied to the data. The space group $P2_1/c$ was chosen based on systematic absences and intensity statistics. This assumption proved to be correct as determined by a successful direct-methods solution [21] and subsequent refinement. All non-hydrogen atoms were placed directly from the E-map and they were refined with anisotropic displacement parameters. The hydrogen atoms were treated as riding-atoms with individual isotropic displacement parameters. The hydrogen atoms on the main body of the molecule were placed from successive difference Fourier maps and refined isotropically. Final refinements were then carried out [21–23]. Selected bond angles and distances are collected in Table 4.

Acknowledgements

The authors are grateful to the Donors of the Petroleum Research Fund administered by the American Chemical Society and the Iowa State Center for Advanced Technology Development for support of this research. We also thank Dr L. Thomas of the Iowa

State Molecular Structure Laboratory for the X-ray structures.

References

[1] (a) J.-S. Tang, J.G. Verkade, Angew. Chem. Int. Ed. Engl. 32 (1993) 896. (b) J.-S. Tang, J.G. Verkade, US Patent No. 5 260 436, 1993; Chem. Abstr. 120, 218836v.
[2] J.-S. Tang, J. Dopke, J.G. Verkade, J. Am. Chem. Soc. 115 (1993) 5015.
[3] J.-S. Tang, J.G. Verkade, Tetrahedron Lett. 34 (1993) 2903.
[4] J.-S. Tang, M.A.H. Laramay, J.G. Verkade, Phosphorus Sulfur Silicon 75 (1993) 205.
[5] (a) J.-S. Tang, J.G. Verkade, J. Org. Chem. 59 (1994) 7793. (b) J.-S. Tang, J.G. Verkade, US Patent No. 5 446 166, Aug. 29, 1995; Chem. Abstr. 123, 83101r.
[6] J.-S. Tang, T. Mohan, J.G. Verkade, J. Org. Chem. 59 (1994) 4931.
[7] T. Mohan, Y. Wan, J.G. Verkade, J. Fluor. Chem. 71 (1995) 185.
[8] A.E. Wroblewski, J. Pinkas, J.G. Verkade, Main Group Chem. 1 (1995) 69.
[9] J.-S. Tang, J.G. Verkade, in: H. Karsch (Ed.), Synthetic Methods in Organometallic and Inorganic Chemistry, vol. 3, 1996, p. 177.
[10] B.A. D'Sa, J.G. Verkade, J. Org. Chem. 61 (1996) 2963.
[11] L. Nyulászi, T. Veszpremi, B.A. D'Sa, J.G. Verkade, Inorg. Chem. 35 (1996) 102.
[12] (a) B.A. D'Sa, J.G. Verkade, J. Am. Chem. Soc. 118 (1996) 12832. (b) B.A. D'Sa, D. McLeod, J.G. Verkade, J. Org. Chem. 62 (1997) 5057.
[13] J.-S. Tang, J.G. Verkade, US Patent No. 5 554 764, 1996; Chem. Abstr. 123, 83101r.
[14] (a) T. Mohan, S. Arumugam, T. Wang, R.A. Jacobson, J.G. Verkade, Heteroatom Chem. 7 (1996) 455. (b) S. Arumugam, J.G. Verkade, J. Org. Chem. 62 (1997) 4827.
[15] J.-S. Tang, J.G. Verkade, J. Org. Chem. 61 (1996) 8750.
[16] Strem Chemical Inc., Newburyport, MA.
[17] (a) J.G. Verkade, Acc. Chem. Res. 26 (1993) 483. (b) J.G. Verkade, Coord. Chem. Rev., Main Group Chemistry Review issue 137 (1994) 233.
[18] S.K. Xi, H. Schmidt, C. Lensink, S. Kim, D. Wintergrass, L.M. Daniels, R.A. Jacobson, J.G. Verkade, Inorg. Chem. 29 (1990) 2214.
[19] M.A.H. Laramay, J.G. Verkade, Z. Anorg. Allg. Chem. 605 (1991) 163.
[20] H. Schmidt, C. Lensink, S.-K. Xi, J.G. Verkade, Zeitschr. Anorg. Allg. Chem. 578 (1989) 75.
[21] SHELXTL-PLUS, Siemens Analytical Xray, Inc., Madison, WI.
[22] SHELXL-93, G.M. Sheldrick, J. Appl. Cryst., in preparation.
[23] All X-ray scattering factors and anomalous dispersion terms were obtained from the International Tables for Crystallography, vol. C, The International Union of Crystallography, Kluwer, Boston, 1995, pp. 4.2.6.8 and 6.1.1.4.